

Large-Scale Growth of High-Quality Hexagonal Boron Nitride Crystals at Atmospheric Pressure from an Fe–Cr Flux

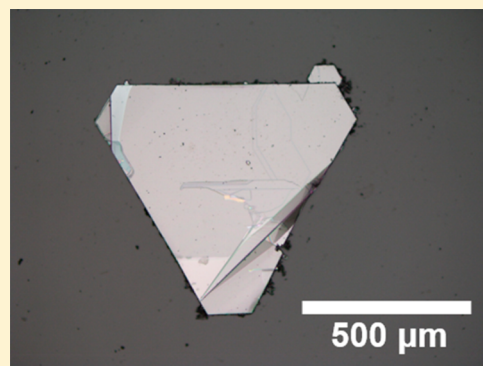
Song Liu,[†] Rui He,[‡] Zhipeng Ye,[‡] Xiaozhang Du,[§] Jingyu Lin,[§] Hongxing Jiang,[§] Bin Liu,[†] and James H. Edgar^{*,†}

[†]Department of Chemical Engineering, Durland Hall, Kansas State University, Manhattan, Kansas 66506, United States

[‡]Department of Physics, University of Northern Iowa, Cedar Falls, Iowa 50614, United States

[§]Department of Electrical and Computer Engineering, Texas Tech University, Lubbock, Texas 79409, United States

ABSTRACT: Single crystals of hexagonal boron nitride (hBN) have recently been envisioned for electronic, optoelectronic, and nanophotonic applications. In this study, the production of large-scale, high-quality hBN single crystals via precipitation from a new solvent composed of Fe and Cr was demonstrated to be viable at atmospheric pressure. The clear and colorless crystals have a maximum domain size of around 2 mm and a thickness of around 200 μm . The Raman spectra and photoluminescence emission spectra demonstrate that the crystals produced with this solvent are pure hBN phase, and with low defect and residual impurity concentrations. The use of an Fe–Cr mixture provides a lower cost alternative to the more common Ni–Cr solvent for growing large hBN of comparable quality.



■ INTRODUCTION

There are many potential applications of hexagonal boron nitride (hBN) that will benefit from high-quality single crystals. These can serve as electrically insulating substrates for epitaxial films, as established for C_{60} ,¹ gallium nitride (GaN),² graphene,^{3–5} molybdenum disulfide (MoS_2),^{6,7} and tungsten disulfide (WS_2).⁸ hBN is also being used as dielectric layers and protective encapsulating layers for graphene^{9,10} and black phosphorus.^{11,12} Single crystals of hBN have a higher breakdown electric fields since they lack grain boundaries present in polycrystalline layers, that are more electrically conductive. Other newly envisioned applications for hBN include ultraviolet light emitting diodes,¹³ neutron detectors,¹⁴ single photon emitters,¹⁵ and nanophotonics.¹⁶ All of these devices will perform their best when fabricated on hBN single crystals.

The best quality hBN single crystals have been precipitated from molten metal solutions. Taniguchi and Watanabe¹⁷ and Zhigadlo¹⁸ produced hBN crystals from solutions at high pressures (>30 kbar). However, crystals of similar quality can also be produced at atmospheric pressure. For example, Kubota et al.¹⁹ first demonstrated atmospheric hBN crystal growth from a Ni–Mo solvent. They reported a Raman peak width of 9.0 cm^{-1} at 1367 cm^{-1} ,¹⁹ which is much narrower than what is typically reported for hBN produced by chemical vapor deposition, i.e., $>15 \text{ cm}^{-1}$.^{20,21} The maximum cathodoluminescence energy of Kubota et al.'s crystals was 5.76 eV.¹⁹

Near atmospheric growth is advantageous, since the crystal growth apparatus is simpler and thus easier to implement at a lower cost. A later study by Kubota et al.²² demonstrated that a

50 wt % mixture of nickel and chromium is an even better solvent for the atmospheric pressure solution growth of hBN single crystals. This alloy succeeds because nickel is a good solvent for boron, with a maximum solubility of 18.5 atom %, ²³ and chromium can dissolve more nitrogen when compared to molybdenum.²⁴

We have previously employed the Ni–Cr flux to produce hBN crystals that were (0001) orientated, a couple of millimeters across and up to 200 μm thick.^{25,26} These crystals had excellent high energy deep ultraviolet photoluminescence spectra with an S-series excitonic emission at 5.897 eV at low temperature.²⁷ They were also sufficiently thick (200 μm) to demonstrate interference-less absorption at infrared frequencies.²⁸

In the present note, we tested whether an iron–chromium solvent can also produce hBN crystals of comparable quality as the Ni–Cr solvent at atmospheric pressure. Like nickel, liquid iron has high comparable boron solubility, 17 atom %.²⁹ The main advantage of iron is that it is less expensive than nickel, by a factor of 5–10.

Prior studies related to steel manufacturing suggest hBN crystal formation from an iron-based alloy should be possible.^{30,31} The joint solubility of boron and nitrogen in iron has been the subject in a number of studies. Fountain and Chipman³⁰ studied these elements in solid iron between 950 and 1150 $^\circ\text{C}$ to understand their impact on the hardenability of

Received: June 21, 2017

Revised: July 31, 2017

Published: August 1, 2017

steel. They reported that the presence of boron enhances nitrogen solubility in solid iron, and the solubility of both elements increases with temperature. For iron with and without boron, the solubility of nitrogen in the solid increased with its partial pressure. Morita et al.³¹ examined the impact of boron on the rate constants for nitrogen incorporation into liquid iron between 1873 and 2023 K. They reported the rate constant for nitrogen decreased with the boron concentration. In contrast, the nitrogen incorporation rate constant increased with the chromium concentration.

In this study, the process of producing hBN crystals from a Fe–Cr flux was developed. The crystal sizes, shapes, and morphologies were determined by optical microscopy. Then the Raman and photoluminescence spectra were taken to assess the quality of the hBN crystals. Comparisons were made of these crystals to previous studies.

EXPERIMENTAL METHODS

hBN Growth. hBN crystals with the natural distribution of isotopes (20% B¹⁰ and 80% B¹¹) were synthesized by precipitation from solution in a high temperature single-zone tube furnace. For one set of crystals, a 50 wt % Fe and 50 wt % Cr powder mixture was loaded into a hot-pressed boron nitride crucible, which was both the source for the boron nitride and the container for the solution. For the other set, a 50 wt % Ni and 50 wt % Cr powder mixture was used. The crucible with the source materials was then transferred into the furnace. The reaction tube was evacuated, and then filled with N₂ and forming gas (5% hydrogen in balance argon) to a constant pressure of 850 Torr. In this experiment, the forming gas was used to minimize oxygen and carbon impurities that are recognized as the main contaminants in hBN crystals. During the reaction, the N₂ and forming gases continuously flowed through the system at rates of 125 and 25 sccm, respectively. The liquid solution was formed by heating the furnace up to 1550 °C and holding for a dwell period of 24 h. The hBN crystals were then precipitated by cooling at a rate of 1 °C/h to 1500 °C. After growth, the system was quickly quenched to room temperature.

Photoluminescence (PL) Measurement. The room temperature PL measurement system includes a frequency-quadruped Ti-sapphire laser with wavelength of 195 nm, 76 MHz repetition rate, 100 fs pulse width, and average optical power of ~1 mW. The emitted light was collected with a 1.3 m-long monochromator onto a microchannel plate photomultiplier tube.

Raman Measurement. Raman spectra were taken at room temperature using a Horiba LabRAM HR Raman microscope system. Our spectrometer is equipped with an ultralow frequency filter that allows access down to ~5 cm⁻¹. A linearly polarized 532 nm laser light was used. It was focused to a spot of ~2 μm diameter by a 50× long-working-distance objective lens. The laser power was kept below 0.8 mW. Instrument resolution was ~0.5 cm⁻¹ by using the 1800 groove/mm grating.

RESULTS AND DISCUSSION

Figure 1a is an optical image of hBN crystals on the solidified Fe–Cr solvent, showing that the grown hBN crystals are clear and colorless. There are two main crystal shapes on the metal surface: hexagonal and triangular. The largest domain is more than 2 mm across. The edge-on view of hBN crystal, as shown in Figure 1b, illustrates that the crystal thickness is around 200 μm. Both crystal size and thickness are comparable with our previous prepared hBN crystals from Ni–Cr solvent. Figure 1c shows an optical micrograph of hBN flake transferred from the metal surface onto a glass substrate, which has a dimension of about 1 mm across.

A comparison of the Raman spectrum for the hBN crystals grown with the Fe–Cr (top) and Ni–Cr (bottom) flux is

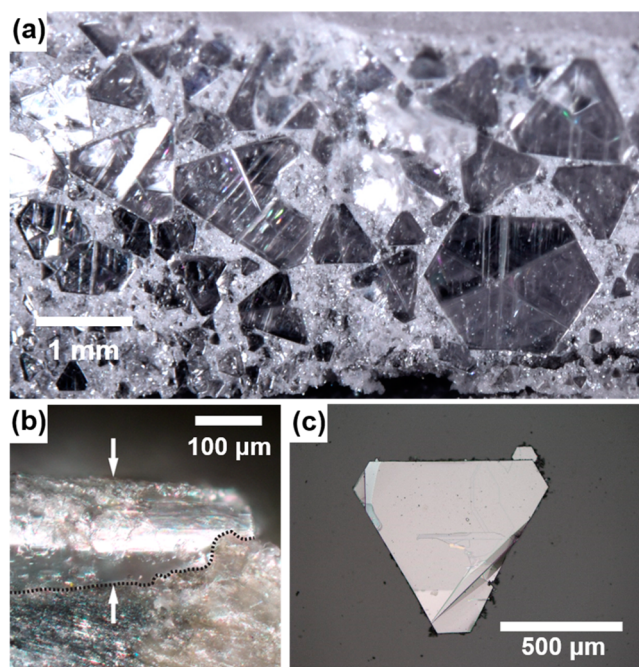


Figure 1. Optical micrograph of (a) hBN crystals on Fe–Cr ingot top surface, (b) edge-on view of hBN crystal thickness, and (c) hBN flake transferred from ingot onto the substrate.

shown in Figure 2. The low-frequency spectrum in Figure 2a, which is attributed to the rigid shearing oscillation between

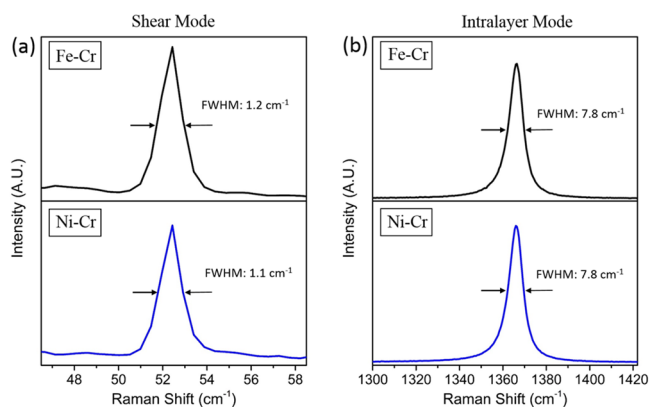


Figure 2. Raman spectra of shear mode (a) and intralayer mode (b) from hBN crystals grown with Fe–Cr (top) and Ni–Cr (bottom) flux.

adjacent layers, shows that hBN crystals from both solvents have an intense peak at same position of 52.5 cm⁻¹, which is consistent with previously reported references.^{32,33} The full width at half-maximum (fwhm) values for the two peaks are respectively 1.2 and 1.1 cm⁻¹, which indicates our hBN crystals are of high quality. The high-frequency spectra in Figure 2b, which corresponds to the intralayer E_{2g} vibrational mode between in-plane boron and nitrogen, show that hBN crystal grown from Fe–Cr has an intense peak at 1366.1 cm⁻¹ with an fwhm of 7.8 cm⁻¹, which is among the smallest values reported in the literature.^{34,35} This is also comparable to our previously prepared high-quality hBN from Ni–Cr flux, which has a consistent peak position and fwhm value, as shown in Figure 2b.

Figure 3 shows the room temperature band-edge PL emission spectra of hBN crystals grown with Fe–Cr and Ni–

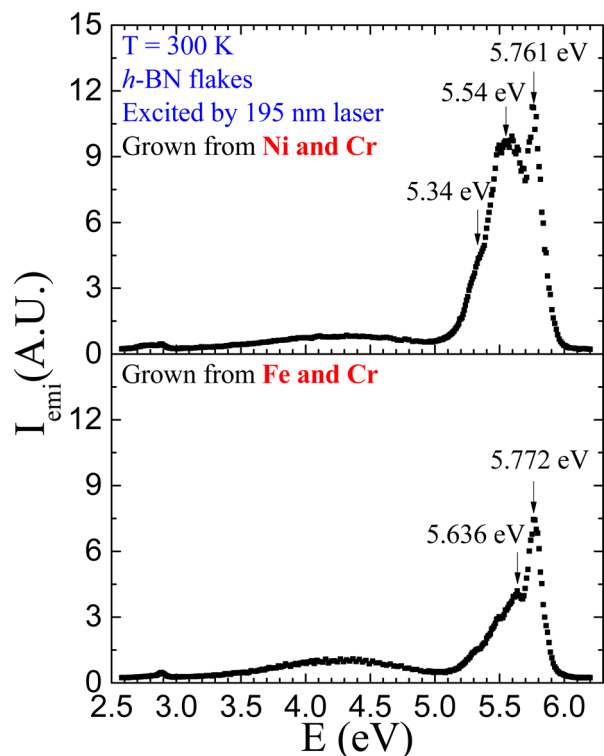


Figure 3. Room temperature PL spectrum comparing hBN crystals growth from (bottom) Fe–Cr and (top) Ni–Cr flux.

Cr solvents. The intense ultraviolet luminescence peaks of the Fe–Cr prepared crystal were at 5.772 and 5.636 eV, which is characteristic of a high-purity, high-quality hBN crystal.²⁷ The slightly higher energy compared to the hBN crystals from Ni–Cr solvent at respective 5.761 and 5.54 eV indicates a better crystal quality. Intensity for energy bands responsible for defects and impurities, located around 4.3 and 2.9 eV, were relatively weak in intensity, confirming a low residual impurity concentration in those crystals. Further investigations will be conducted to quantify the impurity concentration.

CONCLUSIONS

This study demonstrates that large-scale, high-quality bulk hBN single crystals can be successfully formed from a new Fe–Cr solvent at atmospheric pressure. The hBN crystals produced this way are clear and colorless, and have a maximum domain size of around 2 mm with a thickness of around 200 μm , which is comparable with the crystals grown from Ni–Cr solvent. The Raman spectrum of both shear mode and intralayer mode shows the high quality of the crystals. The band-edge PL emission spectra also indicate that the crystals from Fe–Cr have a high quality and low defect and impurity density. Consequently, we have established an alternative growth route for large-scale, high-quality hBN crystals under atmospheric pressure with much lower cost.

AUTHOR INFORMATION

Corresponding Author

*E-mail: edgarjh@ksu.edu.

ORCID

Song Liu: 0000-0002-3046-3335

Bin Liu: 0000-0001-7890-7612

Notes

The authors declare no competing financial interest.

ACKNOWLEDGMENTS

Support from the Materials Engineering and Processing Program of the National Science Foundation, Award Number CMMI 1538127, and the II–VI Foundation is greatly appreciated. The Raman measurement at University of Northern Iowa was supported by the National Science Foundation (NSF CAREER Grant No. DMR-1552482). The work at Texas Tech University was supported by ARO (W911NF-16-1-0268) and monitored by Dr. Michael Gerhold.

REFERENCES

- (1) Lee, T. H.; Kim, K.; Kim, G.; Park, H. J.; Scullion, D.; Shaw, L.; Kim, M.; Gu, X.; Bae, W.; Santos, E. J.; Lee, Z.; Shin, H. S.; Nishi, Y.; Bao, Z. Chemical Vapor-Deposited Hexagonal Boron Nitride as a Scalable Template for High-Performance Organic Field-Effect Transistors. *Chem. Mater.* **2017**, *29*, 2341–2347.
- (2) Kobayashi, Y.; Kumakura, K.; Akasaka, T.; Makimoto, T. Layered boron nitride as a release layer for mechanical transfer of GaN-based devices. *Nature* **2012**, *484*, 223–227.
- (3) Garcia, J. M.; Wurstbauer, U.; Levy, A.; Pfeiffer, L. N.; Pinczuk, A.; Plaut, A. S.; Wang, L.; Dean, C. R.; Buizza, R.; Van Der Zande, A. M.; Hone, J.; Watanabe, K.; Taniguchi, T. Graphene growth on h-BN by molecular beam epitaxy. *Solid State Commun.* **2012**, *152*, 975–978.
- (4) Hwang, B.; Hwang, J.; Yoon, J. K.; Lim, S.; Kim, S.; Lee, M.; Kwon, J. H.; Baek, H.; Sung, D.; Kim, G.; Hong, S.; Ihm, J.; Strosio, J. A.; Kuk, Y. Energy Bandgap and Edge States in an Epitaxially Grown Graphene/h-BN Heterostructure. *Sci. Rep.* **2016**, *6*, 31160.
- (5) Cheng, T. S.; Davies, A.; Summerfield, A.; Cho, Y.; Cebula, I.; Hill, R. J.; Mellor, C. J.; Khlobystov, A. N.; Taniguchi, T.; Watanabe, K.; Beton, P. H.; Foxon, C. T.; Eaves, L.; Novikov, S. V. High temperature MBE of graphene on sapphire and hexagonal boron nitride flakes on sapphire. *J. Vac. Sci. Technol., B: Nanotechnol. Microelectron.: Mater., Process., Meas., Phenom.* **2016**, *34*, 02L101.
- (6) Yan, A.; Velasco, J., Jr.; Kahn, S.; Watanabe, K.; Taniguchi, T.; Wang, F.; Crommie, M. F.; Zettl, A. Direct growth of single- and few-layer MoS₂ on h-BN with preferred relative rotation angles. *Nano Lett.* **2015**, *15*, 6324–6331.
- (7) Wan, Y.; Zhang, H.; Wang, W.; Sheng, B.; Zhang, K.; Wang, Y.; Song, Q.; Mao, N.; Li, Y.; Wang, X.; Zhang, J.; Dai, L. Origin of Improved Optical Quality of Monolayer Molybdenum Disulfide Grown on Hexagonal Boron Nitride Substrate. *Small* **2016**, *12*, 198–203.
- (8) Okada, M.; Sawazaki, T.; Watanabe, K.; Taniguchi, T.; Hibino, H.; Shinohara, H.; Kitaura, R. Direct chemical vapor deposition growth of WS₂ atomic layers on hexagonal boron nitride. *ACS Nano* **2014**, *8*, 8273–8277.
- (9) Petrone, N.; Chari, T.; Meric, I.; Wang, L.; Shepard, K. L.; Hone, J. Flexible graphene field-effect transistors encapsulated in hexagonal boron nitride. *ACS Nano* **2015**, *9*, 8953–8959.
- (10) Hui, F.; Pan, C.; Shi, Y.; Ji, Y.; Grustan-Gutierrez, E.; Lanza, M. On the use of two dimensional hexagonal boron nitride as dielectric. *Microelectron. Eng.* **2016**, *163*, 119–133.
- (11) Constantinescu, G. C.; Hine, N. D. Multipurpose black-phosphorus/hBN heterostructures. *Nano Lett.* **2016**, *16*, 2586–2594.
- (12) Viti, L.; Hu, J.; Coquillat, D.; Politano, A.; Consejo, C.; Knap, W.; Vitiello, M. S. Heterostructured hBN-BP-hBN Nanodetectors at Terahertz Frequencies. *Adv. Mater.* **2016**, *28*, 7390–7396.
- (13) Dahal, R.; Li, J.; Majety, S.; Pantha, B.; Cao, X.; Lin, J.; Jiang, H. Epitaxially grown semiconducting hexagonal boron nitride as a deep ultraviolet photonic material. *Appl. Phys. Lett.* **2011**, *98*, 211110.

- (14) Maity, A.; Doan, T.; Li, J.; Lin, J.; Jiang, H. Realization of highly efficient hexagonal boron nitride neutron detectors. *Appl. Phys. Lett.* **2016**, *109*, 072101.
- (15) Bourrellier, R.; Meuret, S.; Tararan, A.; Stéphan, O.; Kociak, M.; Tizei, L. H.; Zobelli, A. Bright UV single photon emission at point defects in h-BN. *Nano Lett.* **2016**, *16*, 4317–4321.
- (16) Caldwell, J. D.; Kretinin, A.; Chen, Y.; Giannini, V.; Fogler, M. M.; Francescato, Y.; Ellis, C. T.; Tischler, J. G.; Woods, C. R.; Giles, A. J.; Hong, M.; Watanabe, K.; Taniguchi, T.; Maier, S. A.; Novoselov, K. S. Sub-diffractive, volume-confined polaritons in a natural hyperbolic material: hexagonal boron nitride. *Nat. Commun.* **2014**, *5*, 5221.
- (17) Taniguchi, T.; Watanabe, K. Synthesis of high-purity boron nitride single crystals under high pressure by using Ba–BN solvent. *J. Cryst. Growth* **2007**, *303*, 525–529.
- (18) Zhigadlo, N. Crystal growth of hexagonal boron nitride (hBN) from Mg–B–N solvent system under high pressure. *J. Cryst. Growth* **2014**, *402*, 308–311.
- (19) Kubota, Y.; Watanabe, K.; Tsuda, O.; Taniguchi, T. Deep ultraviolet light-emitting hexagonal boron nitride synthesized at atmospheric pressure. *Science* **2007**, *317*, 932–934.
- (20) Ahmed, K.; Dahal, R.; Weltz, A.; Lu, J.; Danon, Y.; Bhat, I. Growth of hexagonal boron nitride on (111) Si for deep UV photonics and thermal neutron detection. *Appl. Phys. Lett.* **2016**, *109*, 113501.
- (21) Li, X.; Jordan, M. B.; Ayari, T.; Sundaram, S.; El Gmili, Y.; Alam, S.; Alam, M.; Patriarache, G.; Voss, P. L.; Salvestrini, J. P.; Ougazzaden, A. Flexible metal-semiconductor-metal device prototype on wafer-scale thick boron nitride layers grown by MOVPE. *Sci. Rep.* **2017**, *7*, 786.
- (22) Kubota, Y.; Watanabe, K.; Tsuda, O.; Taniguchi, T. Hexagonal Boron Nitride Single Crystal Growth at Atmospheric Pressure Using Ni–Cr Solvent. *Chem. Mater.* **2008**, *20*, 1661–1663.
- (23) Portnoi, K.; Romashov, V.; Chubarov, V.; Levinskaya, M. K.; Salibekov, S. Phase diagram of the system nickel-boron. *Powder Metall. Met. Ceram.* **1967**, *6*, 99–103.
- (24) Kowanda, C.; Speidel, M. Solubility of nitrogen in liquid nickel and binary Ni–X_i alloys (X_i = Cr, Mo, W, Mn, Fe, Co) under elevated pressure. *Scr. Mater.* **2003**, *48*, 1073–1078.
- (25) Hoffman, T. B.; Clubine, B.; Zhang, Y.; Snow, K.; Edgar, J. H. Optimization of Ni–Cr flux growth for hexagonal boron nitride single crystals. *J. Cryst. Growth* **2014**, *393*, 114–118.
- (26) Edgar, J. H.; Hoffman, T. B.; Clubine, B.; Currie, M.; Du, X.; Lin, J.; Jiang, H. Characterization of bulk hexagonal boron nitride single crystals grown by the metal flux technique. *J. Cryst. Growth* **2014**, *403*, 110–113.
- (27) Cao, X.; Clubine, B.; Edgar, J.; Lin, J.; Jiang, H. Two-dimensional excitons in three-dimensional hexagonal boron nitride. *Appl. Phys. Lett.* **2013**, *103*, 191106.
- (28) Baranov, D.; Edgar, J. H.; Hoffman, T.; Bassim, N.; Caldwell, J. D. Perfect interferenceless absorption at infrared frequencies by a van der Waals crystal. *Phys. Rev. B: Condens. Matter Mater. Phys.* **2015**, *92*, 201405.
- (29) Kubaschewski, O. *Iron—Binary Phase Diagrams*; Springer-Verlag: Berlin Heidelberg, 1982; pp 15–17.
- (30) Fountain, R.; Chipman, J. Solubility and precipitation of boron nitride in iron-boron alloys. *Trans. Metall. Soc. AIME* **1962**, *224*, 599–605.
- (31) Morita, K.; Hirosumi, T.; Sano, N. Effects of aluminum, silicon, and boron on the dissolution rate of nitrogen into molten iron. *Metall. Mater. Trans. B* **2000**, *31*, 899–904.
- (32) Kuzuba, T.; Era, K.; Ishii, T.; Sato, T. A low frequency Raman-active vibration of hexagonal boron nitride. *Solid State Commun.* **1978**, *25*, 863–865.
- (33) Pakdel, A.; Bando, Y.; Golberg, D. Nano boron nitride flatland. *Chem. Soc. Rev.* **2014**, *43*, 934–959.
- (34) Gorbachev, R. V.; Riaz, I.; Nair, R. R.; Jalil, R.; Britnell, L.; Belle, B. D.; Hill, E. W.; Novoselov, K. S.; Watanabe, K.; Taniguchi, T.; Geim, A. K.; Blake, P. Hunting for monolayer boron nitride: optical and Raman signatures. *Small* **2011**, *7*, 465–468.
- (35) Nemanich, R.; Solin, S.; Martin, R. M. Light scattering study of boron nitride microcrystals. *Phys. Rev. B: Condens. Matter Mater. Phys.* **1981**, *23*, 6348–6356.